Supporting Information for Interpreting the Density of States Extracted from Organic Solar Cells using Transient Photocurrent Measurements.

Roderick C. I. MacKenzie[*ab] , Chris G. Shuttle[c] , George F. Dibb[d] ,Neil Treat[c] , Elizabeth von Hauff[e] , Maxwell J. Robb[f] , Craig J. Hawker[f] , Michael L. Chabinyc[c] and Jenny Nelson[db]

a)Faculty of Engineering, University of Nottingham, Nottingham, Nottinghamshire, NG7 2RD (UK)

b)FRIAS, School of Soft Matter Research, University of Freiburg, Albertstraβe 19, 79104 Freiburg, Germany

c)Materials Department, University of California Santa Barbara, Santa Barbara CA 93106-5050

d)Department of Physics, Imperial College London, South Kensington Campus, London, SW7 2AZ (UK)

e)Institute of Physics, Hermann-Herder-Str. 3a D-79104, Freiburg, Germany

f)Materials Research Laboratory, University of California, Santa Barbara, CA 93106-5121

*e-mail: roderick.mackenzie@nottingham.ac.uk, Tel: (+44) 01157484434

1.1 Experimental Details

Synthesis:

PDPP2FT was prepared according to a modified literature procedure[1]. DPP2FT-Br2 monomer (0.161 g, 0.247 mmol), 2,5-bis(trimethylstannyl) thiophene (0.101 g, 0.247 mmol), Pd2dba3 (2 mol%), and P(o-tolyl)3 (8 mol %) were combined with 5.0 mL of chlorobenzene in a 10 mL microwave vial and subsequently sealed with a teflon crimp cap. The solution was sparged with argon for 20 min followed by heating to 180 ^{0}C for 45 min in a CEM microwave reactor at a power of 250 W. After cooling, the reaction mixture was diluted with 4 mL of chlorobenzene, precipitated into 400 mL of methanol, and the crude polymer was isolated by vacuum filtration. The polymer was treated by Soxhlet extraction with methanol (overnight) and hexane (2 hr) and further purified by passing a solution of the polymer in chloroform through a short plug of silica, neutral alumina, and celite (1:1:1). The eluate was concentrated by rotary evaporation, precipitated into 400 mL of methanol, and isolated by vacuum filtration, resulting in 0.141 g of a dark colored polymer after drying under vacuum. Molecular weights and molecular weight distributions were determined by GPC in chloroform relative to polystyrene standards: M_n = 49 kDa; PDI = 3.95.

Fabrication of Solar Cells:

ITO-coated glass substrates were ultrasonicated in acetone, 2% soap in water, deionized water, and 2-propanol for 20 min and dried with nitrogen. A 40 nm thick film of PEDOT:PSS (Clevios PVP Al 4083) was deposited by spin coating at 4000 rpm for 40 s and dried at 165°C for 10 min.

The PDPP2FT and PC71BM stock solutions were prepared in chlorobenzene in a N 2 glove box at a concentration of 15 mg/mL and 45 mg/mL respectively, stirred overnight at 80°C and filtered with a 0.45 μm PTFE filter prior to use. All devices were fabricated with a weight ratio for PDPP2FT:PC71BM of 1:3 with 9 % vol CN. These solutions were spin coated at 1200 rpm for 40 s and then at 2000 rpm for 5 s on the prepared substrates. The electrodes were then evaporated under vacuum (10^{-6} torr). Lithium fluoride was typically evaporated at a rate of 0.15 Å/s for a final thickness of 1.5 nm. Aluminum was typically Å/s with a final thickness of 75 nm. Each substrate contained 5 solar cells evaporated at a rate of 3 Å with an area of 0.06 cm2 . The J-V characteristics (figure S1) were measured at 1 sun (AM 1.5G) in a N_2 filled glove box equipped with a Xenon lamp (Newport) and Keithley 2408 SMU. The fabrication of the P3HT:PCBM can be found in 10.1063/1.2891871. The procedure was altered to use 35mg/ml in 1.5:1 P3HT: PC(60)BM in chlorobenzene.

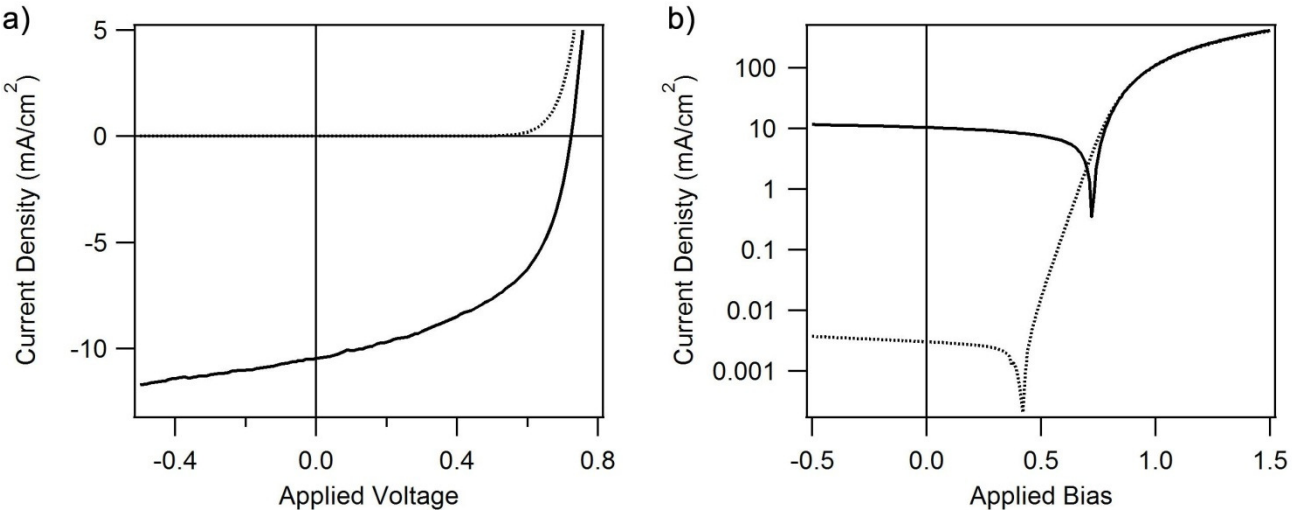

Figure S1: (a) Linear and log (b) scale light (black) and dark (grey) current-voltage characteristics of PDPP2FT:PC71BM solar cells. Low-level background light leakage caused the small photocurrent observed in the dark characteristic.

1.2 The model parameters

Mechanism	Symbol	Value
Left contact electron density	n_l	$9.0x10^{25}$ m^{-3}
Right contact hole density	p_r	$9.0x10^{25}$ m^{-3}
Effective electron trap density	N^{exp}_e	$5.0x10^{25}$ m^{-3} eV^{-1}
Effective hole trap density	N^{exp}_h	$5.0x10^{25}$ m^{-3} eV^{-1}
Characteristic energy for electron exponential tail	E^u_e	60 meV
Characteristic energy for hole exponential tail	E^u_h	100 meV
Effective density of free electron states	N_c	$1x10^{26}$ m^{-3}
Effective density of free hole states	N_v	$1x10^{26}$ m^{-3}
LUMO electron capture cross section	σ^e_e	$1x10^{-21}$ m^{-2}
LUMO hole capture cross section	σ^e_h	$1x10^{-22}$ m^{-2}
HOMO electron capture cross section	σ^e_h	$1x10^{-22}$ m^{-2}
HOMO hole capture cross section	σ^h_h	$1x10^{-21}$ m^{-2}
Free electron mobility	μ_{e0}	$1x10^{-5}$ m^2 V^{-1} s^{-1}
Free hole mobility	μ_{h0}	$1x10^{-5}$ m^2 V^{-1} s^{-1}
Shunt resistance	R_{shunt}	$1.902x10^5$ Ω
Contact resistance	$R_{contact}$	19.5 Ω
Thermal velocity	v_{th}	$1.0x10^5$ m s^{-1}
LUMO mobility edge	E^d_e	−3.8 eV
HOMO mobility edge	E^d_h	−4.9 eV
Cell thickness	L	220 nm

Table S1: Generic simulation parameters.

1.3 Dynamic voltage dependent features in the DoS

To investigate the influence recombination has on the extracted DoS at negative voltages, the electron and hole cross sections were set equal and varied together, the results plotted in figure S2. As the capture cross sections are increased (higher recombination) the extracted DoS shortens, this is due to recombination removing long lived carriers from deep traps, this process is also visible in figure 8 between 0.57 - 0.60 eV in the hole distribution. High recombination also cause the extracted DoS to flatten out between 0.15 eV and 0.3 eV . With very fast recombination rates a peak can be observed in the DoS within this energy range. This is due to the free carriers of one species being able to move into the trapped states of the other carrier species faster than

moving into its own trapped states during the pre-transit. The bump is then caused by these trapped carriers moving back to the free carrier population. Figure S3 shows the transient with a large capture cross section (1×10^{-19} m^2) simulated with applied biases ranging between 0 V and -2 V . Because carrier thermalization will eliminate holes (electrons) stored in electron (hole) traps the process will be dependent upon the density of free carriers and thus the applied voltage. This can be seen in figure S3 where the magnitude of the Gaussian depends upon the applied voltage. If we compare the simulated results in figure S3 and the experimental data in figure 3 we can see that the same trends can be observed. This suggests that the experimentally observed Gaussian is probably not a deep trap but due to dynamic effects within the device.

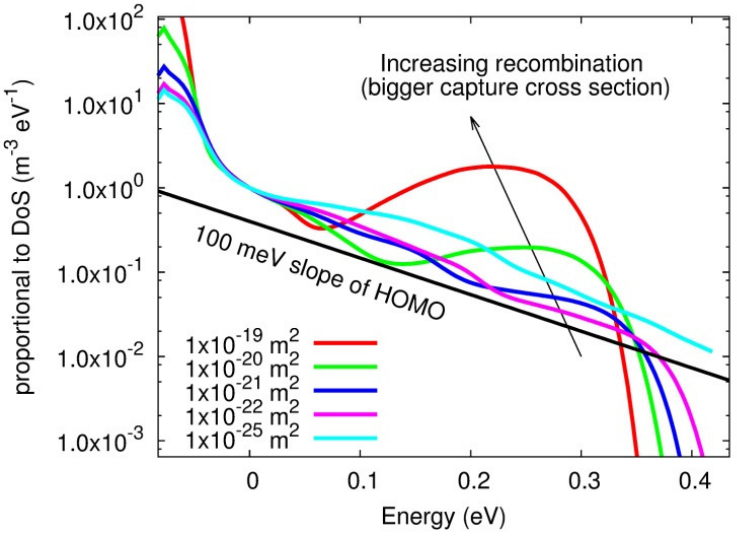

Figure S2: The extracted DoS when the electron (σ_h) and hole (σ_e) recombination cross sections are increased together. With small recombination cross sections the HOMO can be recovered, higher cross sections result in a flattering of the extracted DoS and larger still cross sections result in a bump forming in the extracted DoS.

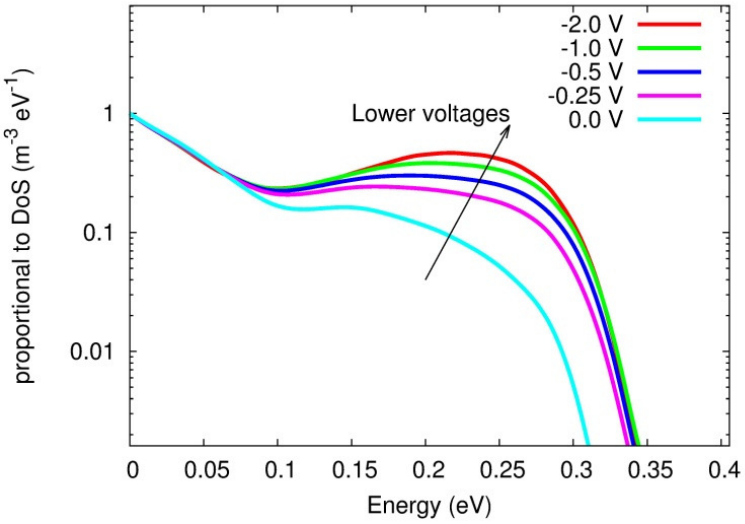

Figure S3: Recombination creating a bump in the extracted DoS, if this were an experimental measurement it would be easy to confuse the feature for a deep trap. However, the fact that the magnitude of the feature changes as a function of voltage suggests it does not originate from the DoS distribution. This voltage dependent behavior can be seen in the experimental data for PCDTBT:PCBM.

References

1. Woo, C. H.; Beaujuge, P. M.; Holcombe, T. W.; Lee, O. P.; Frechet, J. M. J. Incorporation of Furan into Low Band-Gap Polymers for Efficient Solar Cells. *J. Am. Chem. Soc.* **2010**, 132, 15547–15549.